HYDRO-GEOTECHNICAL ROCK SCOUR ASSESSMENT AT PETIT-SAUT DAM

STEVEN E. PELLS[1], FANAR AL-QASSAB[2], FELICIA WEIR[3], ANAÏS FAIVRE[4], THIERRY LETURCQ[5], BENOIT BLANCHER[4]

[1]1 Pells Consulting, 49 Lakeside Drive, MacMasters Beach, NSW, 2251, Australia; e-mail: steven@pellsconsulting.com.au
[2] GHD, Level 15/133 Castlereagh St, Sydney, NSW, 2000, Australia
[3] PSM G3 56 Delhi Road, North Ryde, NSW, 2113, Australia
[4] EDF – Centre d'Ingénierie Hydraulique
[5].EDF - Technique de réalisation, Expertise Géologie Génie Civil

Key words: Scour, Rock, Hydro-geotechnical scour assessment.

Summary. This paper presents a recommended design procedure for assessment of rock scour which is illustrated for the case study of Petit-Saut Dam in French Guiana. The methodology, referred to as a "hydro-geotechnical scour assessment", promotes a multi-discipline approach, applying expertise in both rock mechanics and hydraulics, and guides the diagnosis of scour and response to risk by application of currently available scour assessment techniques.

1 INTRODUCTION

This paper illustrates the practical application of a "hydro-geotechnical scour assessment" methodology. This methodology features a sequence of stages which: guide the assembly and interpretation of available data; give balanced consideration of rock mechanics and hydro-dynamics using current industry practices; assist with the selection of scour assessment methodology, and; guide the assessment of, and appropriate response to, risk. The application of each stage is illustrated for the case study of Petit-Saut Dam, in French Guiana..

2 HYDROGEOTECHNICAL SCOUR ASSESSMENT

A proper assessment of erosion of rock masses must consider both geotechnical and hydraulic factors. A "hydro-geotechnical scour assessment" is a methodology for assessment of erosion of rock masses which provides a framework for applying best practice methods in engineering geology and hydraulics. This methodology is achieved by following the flowchart in Figure 1, which was prepared for the European Group of ICOLD and the French Committee on Dams and Reservoirs following a specialist workshop on spillway scour in Aussois, France, December 2017. The rationale for, and various features of this methodology is discussed in proceedings from this workshop and also in Pells and Douglas, 2019. This methodology guides the systematic collation and assessment of data; encourages synthesis of independent hydraulic and geologic assessments; organizes the currently available scour assessment technologies into separate strands of analysis, and; guides the appropriate response to scour through assessment of risk, mitigations strategies and surveillance.

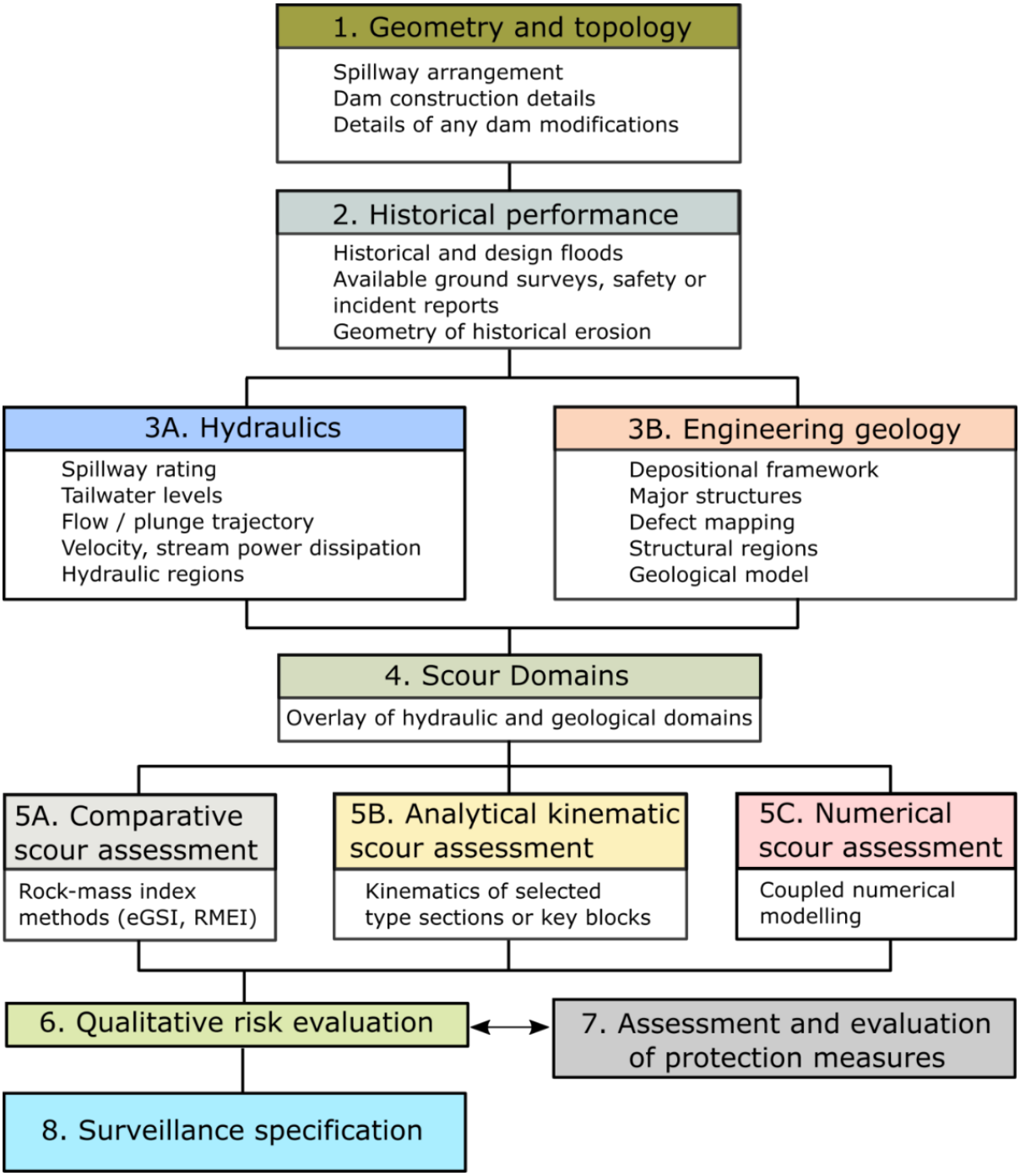

Figure 1: Flow chart for a "hydro-geotechnical scour assessment".

3 HYDROGEOTECHNICAL SCOUR ASSESSMENT OF PETIT-SAUT DAM

"Petit-Saut" ("little step" in English) is a local name for a zone of rapids over a natural rock weir caused by an exposed granite intrusion across this Sinnamary River in French Guiana (5° 3' 45"N, 53° 2' 54"W). The construction of Petit-Saut Dam in February 1995 to meet local hydroelectricity and water supply demands capitalized on this natural geological feature.

3.1 Geometry and topology

The primary dam at Petit-Saut is a roller compacted concrete gravity structure, 740 m long and with crest elevation of 37m NGG and a maximum height 44 m. A photographic overview of the dam is shown in Figure 2. The dam features four (4) outflow locations (Figure 3):

1. Four power plant turbines discharging to the tailrace via a re-oxygenation weir
2. The bottom outlet which features three gated outlets
3. A 60m wide free overflow stepped spillway, located on the left bank.
4. A single 10m wide outlet gate adjacent to the powerplant.

Figure 2: Overview of Petit-Saut Dam (1 July 1995).

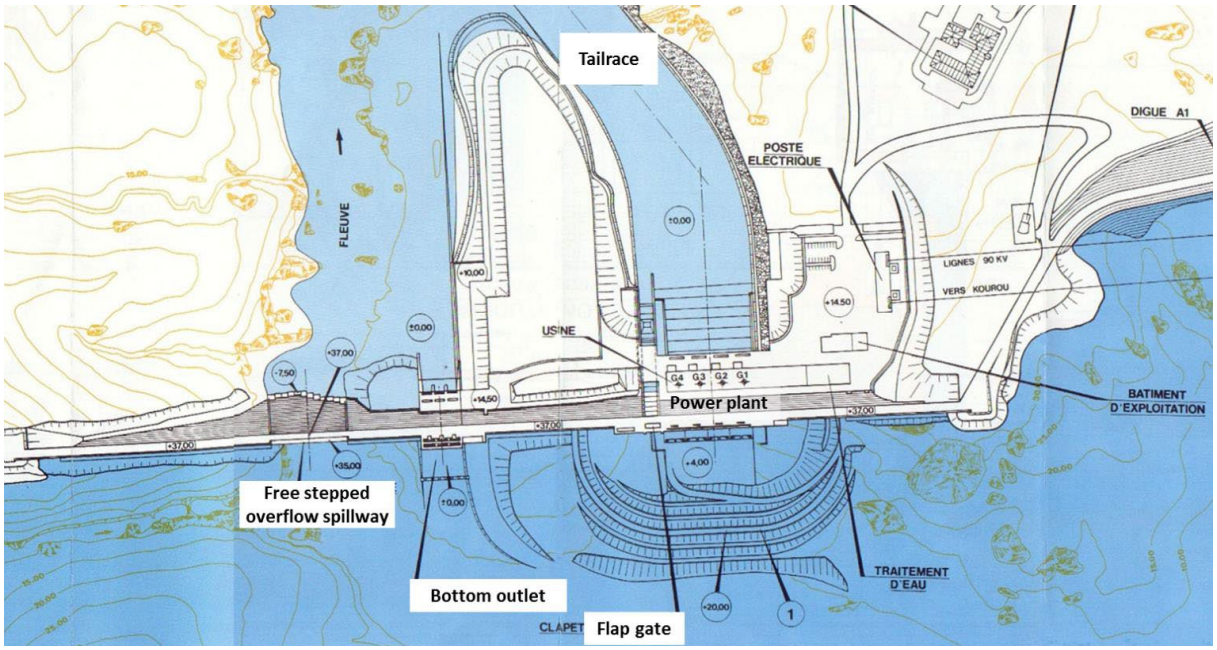

Figure 3: Plan view of the dam and outlet structures.

The bottom outlet is the focus of this paper. It comprises three gated outlets, with numbering convention as shown in Figure 4. Each gated outlet is 7 m width and 6.7 m high. Flow is controlled by sluice gates – there is an upstream guard gate (usually open) and a downstream service gate, which is manipulated to control flows. Whereas the power station discharges are released into a constructed tailrace, flows from the bottom outlet are released to the right bank of the original river channel. A concrete wall retains earth and rock materials on the right bank for a distance of approximately 80 m downstream of the bottom outlet, as seen in Figure 4.

Figure 4: View of bottom outlet (showing numbering convention) and overflow spillway (1 July 1995).

3.2 Historical performance

Flow releases through the bottom outlet have been made typically in response to seasonal flooding. There were regular releases between commissioning of the dam and mid-1997. Large releases in early 2000 corresponded with a large flood at this time. Since 2000 there have been 8 further flow releases, many of them relatively minor. Releases prior to 2015 favoured Gates 1 and 2, whereas releases since that time have been primarily through Gate 3.

As-constructed ground surveys have not been sourced, but it is assumed that, at commissioning, the floor of the chute downstream of the bottom outlets was set at approximately 0m NGG, in accordance with designs. Two bathymetric surveys have since been undertaken, being in November 2014 and November 2017 using a multibeam sounder (Sondeur multifaisceaux R2 Sonic 2022). The bathymetric surveys were rendered as hillshade rasters in Figure 5 below. Long- and cross-sections through the bottom outlet are shown in Figure 6 and Figure 7, respectively. In 2017, in addition to the bathymetric survey, there was a detailed inspection of the cavities / scour holes made with an underwater 3D scanner (Scanner 3D sous-marin BLUEVIEW BV5000).

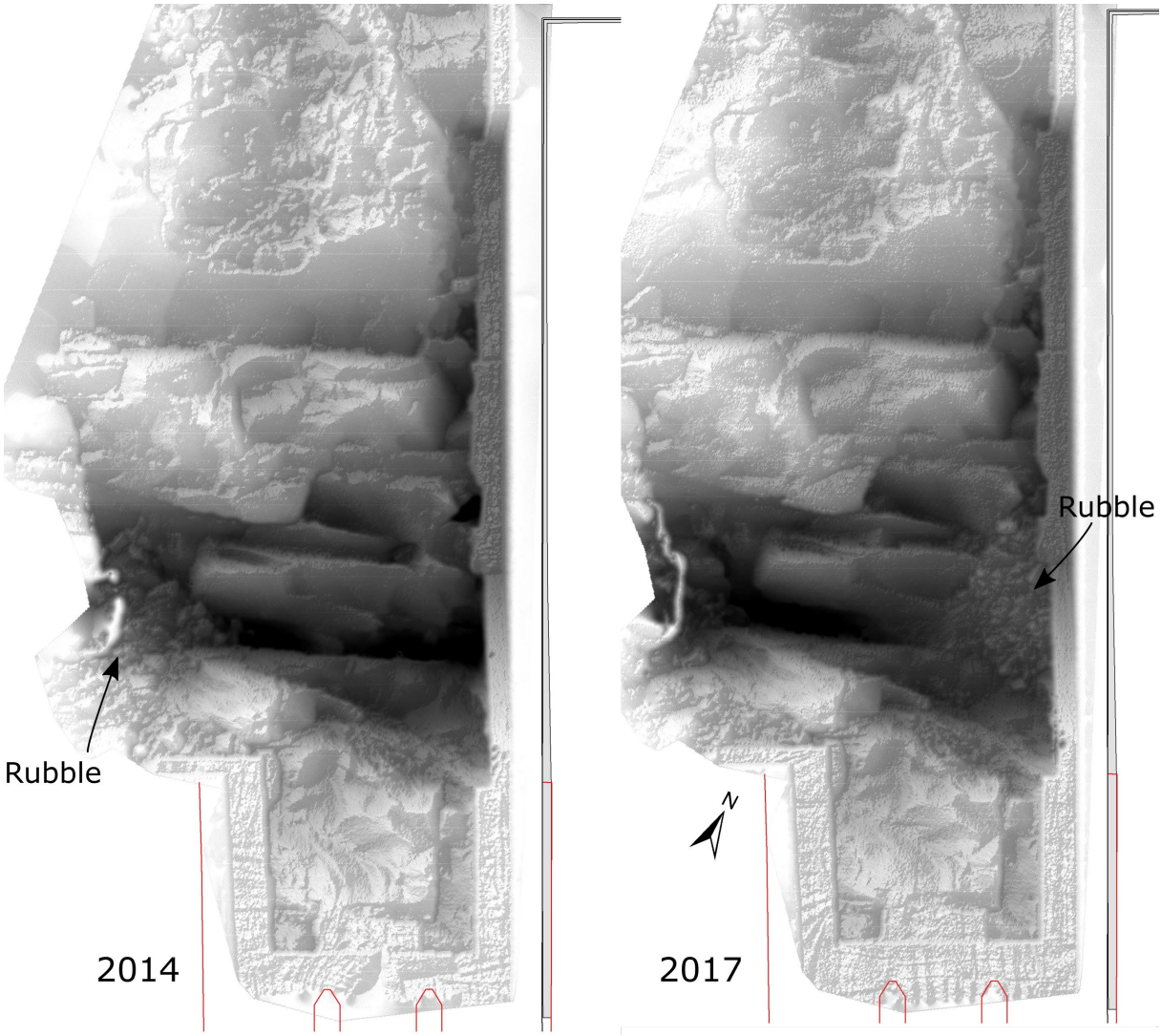

Figure 5: Hill-shade perspectives of bottom outlet bathymetry, November 2014 and November 2017.

The following observations are made:

- The November 2014 survey reveals erosion that has occurred over the 20-year period since commissioning of the dam. This erosion arose from 12 flood seasons and the flood-of-record release in 2000.
- A large scour hole has developed, which has a shape that clearly reveals that rock mass has been removed between persistent subvertical and upstream-dipping joint sets, which strike perpendicular to the flow direction. The upstream dipping defect-surface is interpreted to be sheet-jointing. The remaining rock mass has the appearance of fresh granite, and it is postulated that the scour hole shape reflects the extents of a deeper but localised weathering zone, as is commonly observed in granitic formations.
- Erosion against the retaining wall has revealed the wall footing, reflecting preferential operation of Gate 1 prior to 2014 but may also have been facilitated by rock-mass disturbance from excavation for the wall footing.
- A pile of loose rubble located at the left bank is visible in the 2014 survey, interpreted to be derived from erosion extending laterally into the left-hand bank (**Figure 8**). In the 2017 survey, the rubble adjacent to the left-hand bank was removed with a corresponding accretion of rubble at the right bank in the 2017 survey. This is

considered to be relocation of the same rubble by circulation patterns following the preferential operation of the left-hand gate (number 3) since the 2014 survey.

- The large volume of rock mass eroded prior to 2014 must have been transported downstream. Site photographs show accretion of rocks downstream of the bottom outlet, which may be the eroded material. This is indicative of movement of large intact rock units, perhaps weathered core-stones, rather that erosion of the rock substance.
- The erosion profile in Figure 6 follows the decline of the wall footing, which may indicate the profile of competent rock, as sought and encountered during construction of the wall.
- Comparison between the November 2014 and November 2017 surveys indicates that little additional erosion of the rock mass occurred, despite the occurrence of significant flows.

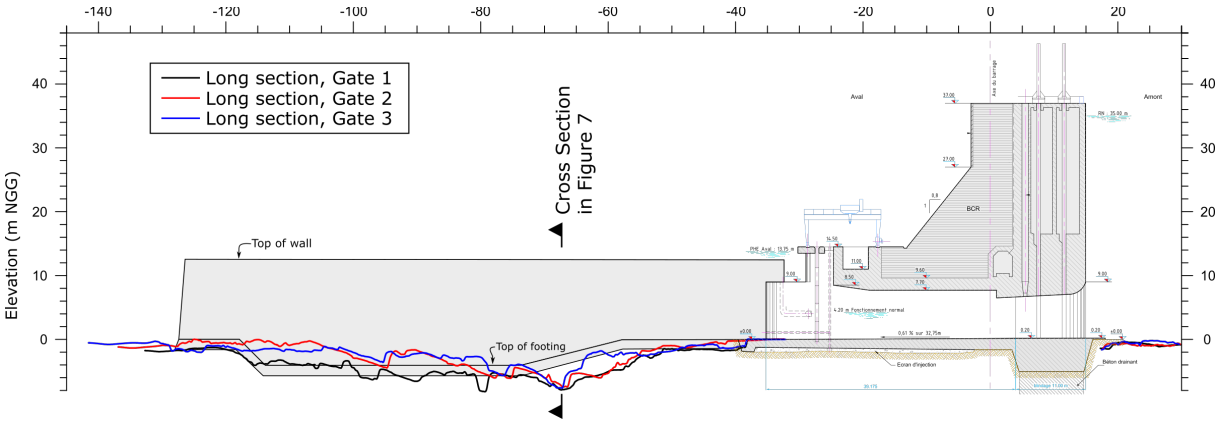

Figure 6: Long section through bottom outlet, 2014 elevation.

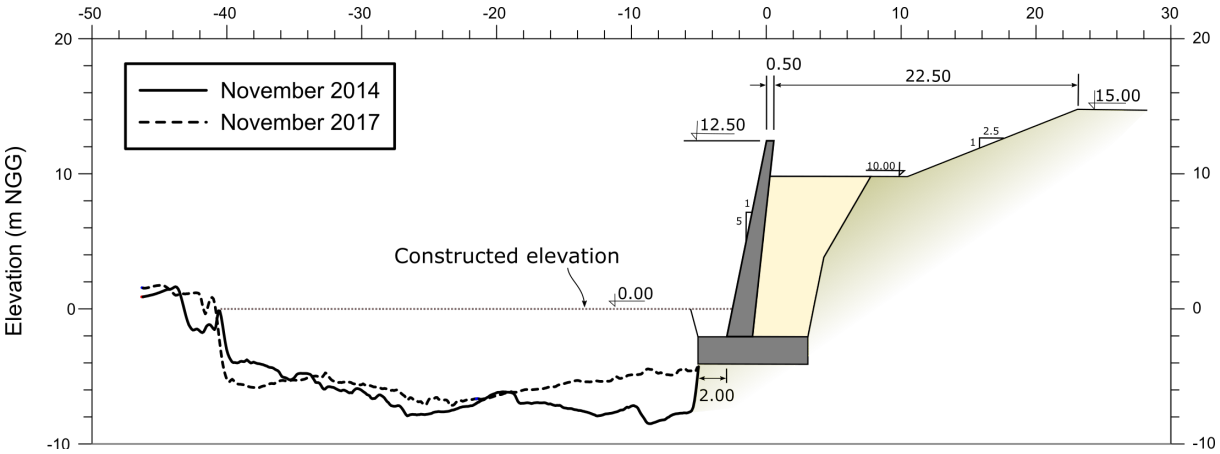

Figure 7: Cross-section through bottom outlet looking downstream, 2014 elevation.

Figure 8: Erosion of the left bank to the bottom outlet (2018).

3.3 Hydraulics

FLOW3D was used to simulate hydraulic conditions through the bottom outlet. FLOW3D is a Computational Fluid Dynamics (CFD) code which provides 3-dimensional analysis of fluid motion by solving the equations governing the conservation of mass, momentum, and energy including the evaluation of turbulence. The CFD model domain was 100m wide by 300m length, encapsulating the bottom outlet from approximately 100m upstream of the dam axis to 200m downstream. A global mesh size of 1m was used but was refined to 0.5m within the outlet and 0.2m around the gates. A "Renormalized Group (RNG)" solution was used for viscosity evaluation. Four model scenarios were run as summarized in Table 1. Selected results showing velocity and flow path tracking are presented in Figure 9, which explains, *inter alia*, the lateral movement of rubble that occurs with different gate operations.

Table 1 : Numerical flow scenarios.

Scenario	Reservoir Level m NGG	Topography	Gate opening			Total discharge $m^3.s^{-1}$
			1	2	3	
1	35	As constructed	50%	-	-	465
2	35	2014	50%	-	-	465
3	35	2014	-	-	50%	465
4	35	2014	100%	100%	100%	3255

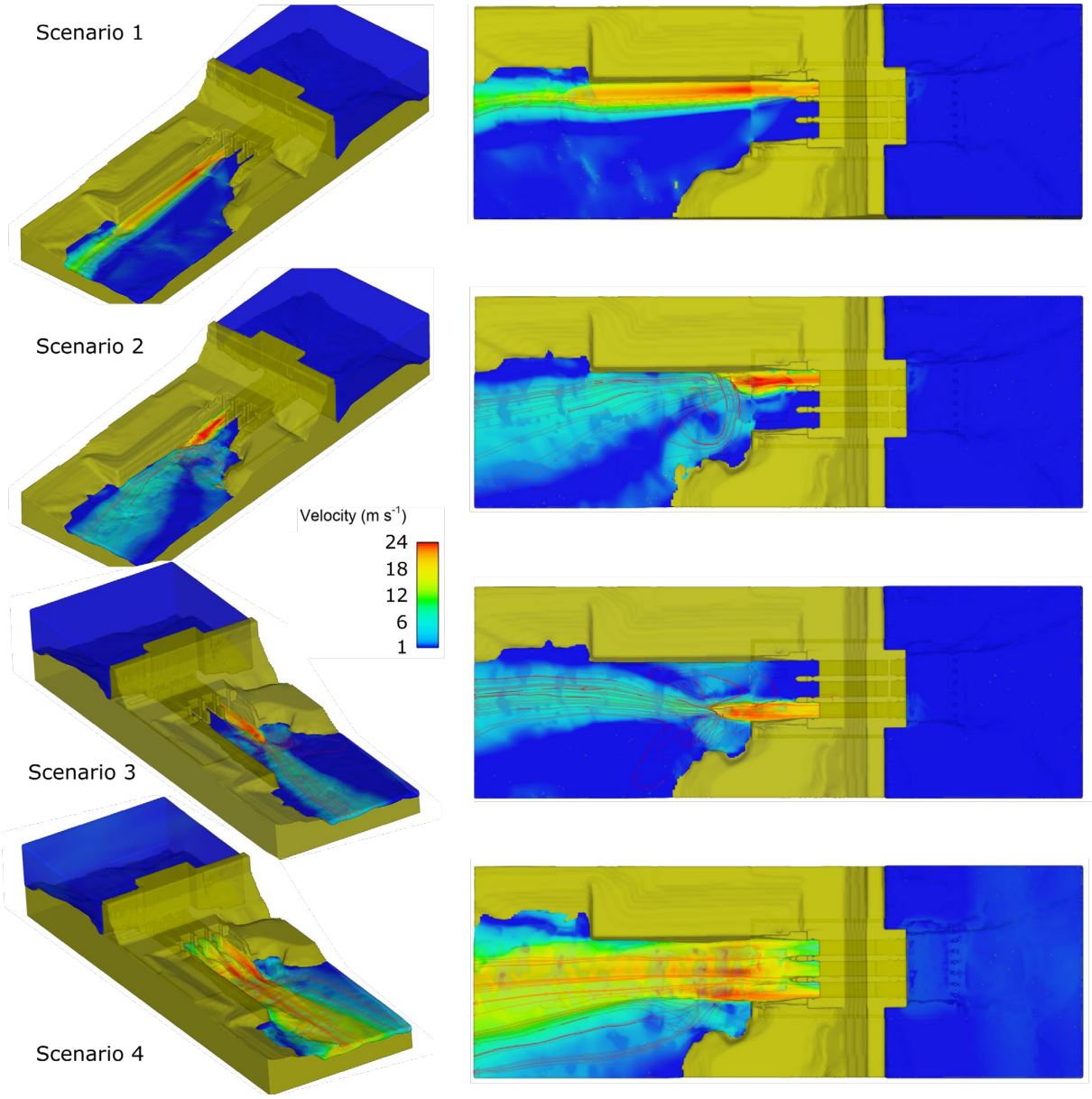

Figure 9: Flow velocity and patterns from CFD modeling.

Unit stream power dissipation (Π_{UD}) (Equation 1) is used in as an index of erosive power in various erosion assessment methods (described in Section 3.6 below).

$$\Pi_{UD} = \rho g \frac{Q}{B}\frac{\Delta H}{\Delta L} = \rho g q S_f \quad (1)$$

where Π_{UD} is the unit stream power dissipation (W.m^{-2}), ρ is the water density (kg/m^3), g is the acceleration due to gravity (m.s^{-2}), Q is the discharge (m^3.s^{-1}), B is the channel width (m), q is the specific discharge (m^2.s^{-1}), $\Delta H/\Delta L$ = the loss in total hydraulic energy head ΔH over a stream-wise distance ΔL= S_f, the gradient of the total energy line.
With substitution for bed shear stress ($\tau_0 = \rho g R_H S_f$), Equation (1) can be expressed as:

$$\Pi_{UD} = q\frac{\tau_0}{R_H} = ud\frac{\tau_0}{R_H} \cong \tau_0 u \quad (2)$$

where R_H hydraulic radius (m), d is the water depth (m), τ_0 is the bed shear stress (kg.m^{-1}.s^{-2}).

FLOW3D does not include in-built functions for directly reporting Π_{UD} so representations of power dissipation were made by post-processing CFD results by various methods including depth-integrating turbulent dissipation and resolving Equations (1) (Figure 10) and Equation (2) (Figure 11) for each computational cell. It is quite a complicated matter resolving Equations 1 and 2 at the cell level and care must be taken to ensure that the energy gradient is resolved in the stream-wise direction and assumptions are applied to represent the specific discharge and the hydraulic radius of a cell. The differences between Figures 10 and 11 relate to these details. These analyses yield detailed maps of stream power dissipation over the spillway domain, and usefully highlight regions of higher hydraulic loading.

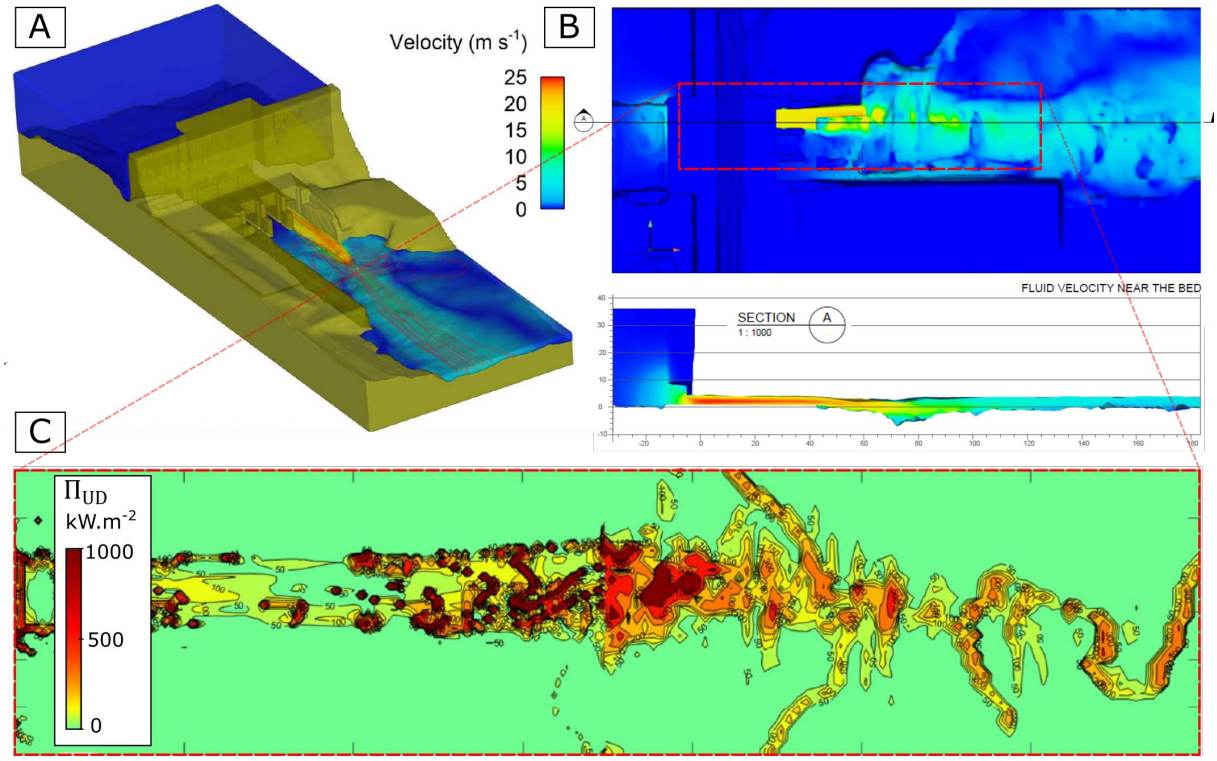

Figure 10: Example of Π_{UD} calculated from CFD results. (A) 3D perspective of the spillway, showing velocities; (B) Plan and sectional view of velocity; (C) Plan view where Equation 1 is applied to each computational cell and values summed through the flow depth.

However, currently published erosion assessment methods that adopt Π_{UD} as an index of erodibility are based on 1D, depth- and time-averaged representations of Π_{UD}. Using these methods, the "hot spots" of high dissipation (eg Figures 10 and 11) suggest localized and severe erosion in places where a corresponding analysis using depth-averaged assumptions show no such risk. To obtain estimates of ΠUD that were compatible with published erosion assessment methods, spatial and temporal averaging of the CFD results was required. For this present study, contours (in plan view) of the total energy head where prepared, which allowed visual estimation of the energy dissipation slope. Estimations of Π_{UD} were made as the product of this energy dissipation slope with specific discharge reported from Flow3D "flux planes". Whilst this methodology does not capitalize on the detail offered by CFD modelling, it is a necessary simplification until further research is undertaken to correlate such detailed Π_{UD} analyses against case data on observed erosion. CFD modelling is nonetheless required in cases such as Petit-Saut outlet to resolve and examine rapidly-varied flow conditions – which 1D analyses cannot do accurately.

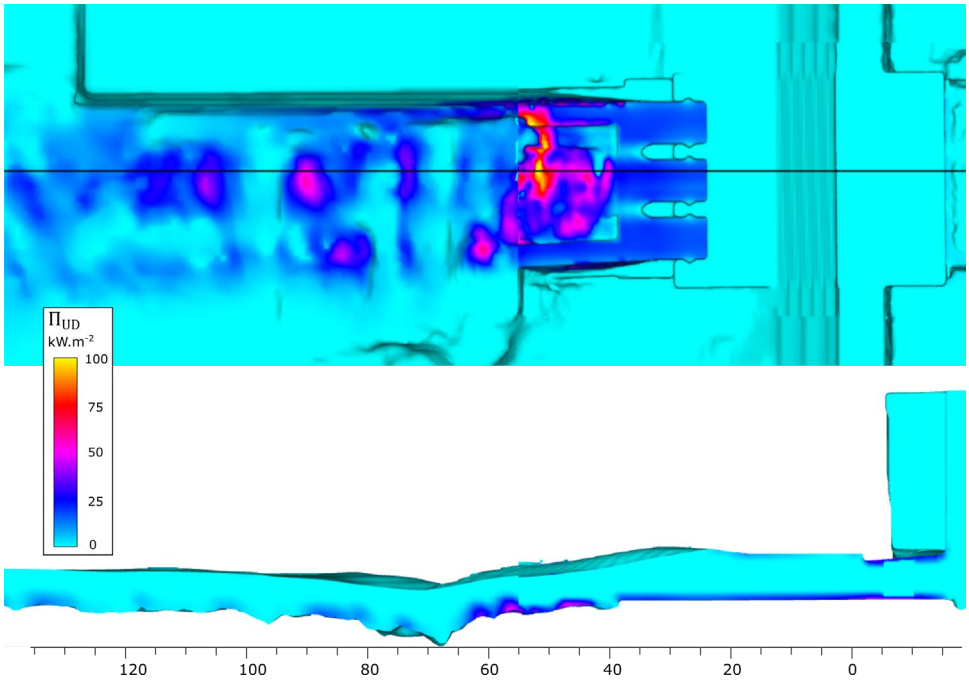

Figure 11: Π_{UD} as the product of shear stress and velocity (Scenario 4).

Five different hydraulic domains (HD) were defined as shown in Figure 12. Assessed hydraulic indices for each HD is presented in Table 2. The following observations are made on the results from FLOW3D:

- Releases from the Gate 1 with the as-constructed topography show the high-velocity jet remaining close to the wall and extending over the excavated section without entering a hydraulic jump. This, along with the possibility of disturbed rock mass adjacent to the retaining wall toe due to excavation for its footings, may explain the elongated extent of erosion observed adjacent to the retaining wall.
- With development of a scour hole, the extent of high velocity flows and high energy dissipation is shortened and focused onto the upstream region.
- The locations of peak hydraulic dissipation are similar for flows from the left hand and right hand gates. The peak hydraulic dissipation extends from the end of the concrete lining and over the upstream edge of the bed-slope descending into the scour hole.
- At many locations, larger discharges associated with wider gate openings do not appear to result in higher unit stream power dissipation values, as the energy is dissipated over a longer distance.

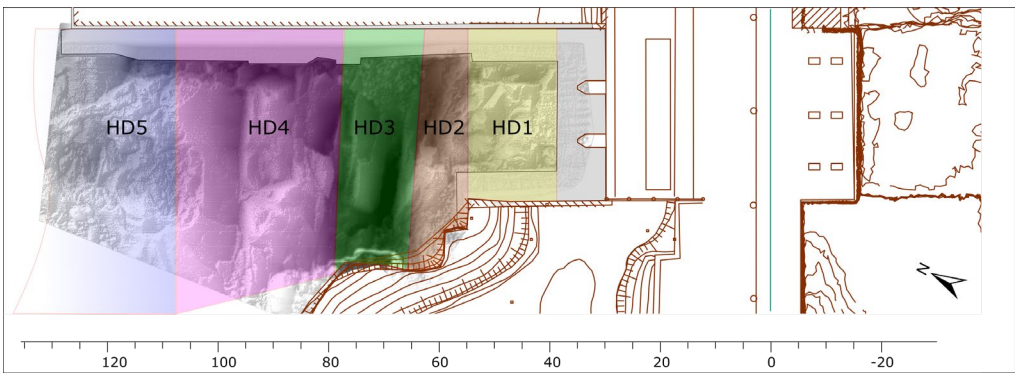

Figure 12: Interpreted hydraulic domains.

Table 2 : Interpreted hydraulic indices for hydraulic domains.

Gate opening amount	Reservoir level	Approx. discharge per gate	Hydraulic Domains	As constructed bathymetry			Eroded bathymetry		
				Velocity	Shear stress	Π_{UD}	Velocity	Shear stress	Π_{UD}
	m NGG	m^3/s		m/s	kPa	kW/m^2	m/s	kPa	kW/m^2
50%	35	400	HD1	22.5	3	140	22.5	3 to 6	140 to 280
			HD2	21	2.7	130	22	2 to 3.5	120 to 160
			HD3	20	2.5	100	14 to 19	1 to 2	40 to 80
			HD4	17	2	60	8 to 10	1 to 1.5	10 to 40
			HD5	15	1.5	40	7 to 8	<1	<20
100%	35	1000	HD1	-	-	-	24	3 to 5	140 to 200
			HD2	-	-	-	21	2 to 3.5	80 to 150
			HD3	-	-	-	19	2 to 2.75	80 to 120
			HD4	-	-	-	19	2 to 3	80 to 120
			HD5	-	-	-	17	1 to 2.5	40 to 80

3.4 Engineering geology

A conceptual engineering geology model for a granitic rock mass, based on experience in similar conditions, is summarised in Figure 13. The primary features are:

- Corestones, rounded boulders of largely unweathered rock in a matrix of weathered soils. They occur individually or in piles as a result of chemical weathering.
- Sheet joints ("onion skin weathering"), which are highly continuous defects that form as a result of stress release. These joints are more closely spaced near the surface and can extend to depths of greater 60m.
- Irregular weathering profile, which is related to preferential weathering along joints (particularly sheet joints) and the development of corestones.

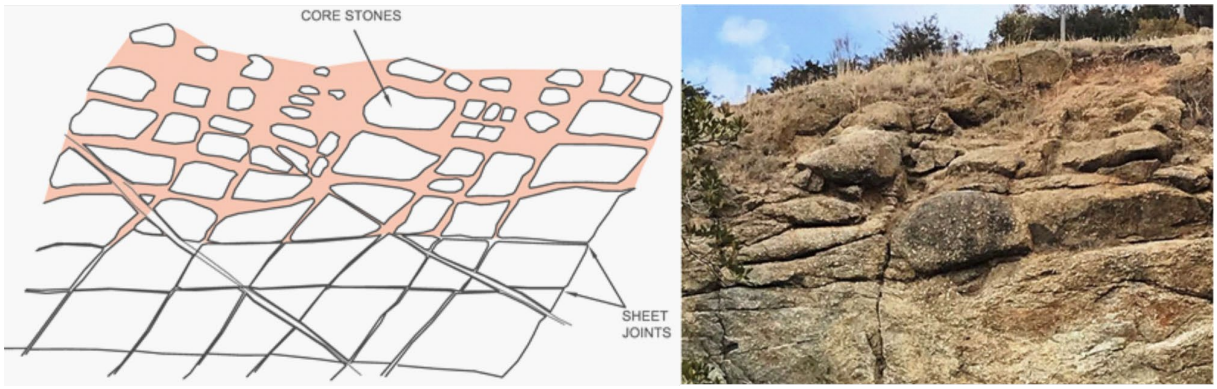

Figure 13: Conceptual engineering geology model for a granitic rock mass.

Geological data were compiled from various sources, including regional geological maps in the public domain and geological reports, site investigations, laboratory measurements, defect measurements, mapping and photographs taken during construction (eg Figures 13 and 14). Based on these data sources, four key engineering geological units were defined: soils (sandy-clay laterites); Highly to Moderately Weathered Granite ("HWG"), Weathered Granite ("WG") and Fresh Jointed Granite ("FG"). The interpreted stratigraphy in the spillway, comprising these geological units, is presented in Figure 15.

Interpretation of Rock Mass Indices were made for each of the engineering geological

units, selecting those systems previous published as indicators of erodibility (eg Kirsten Index, after Kirsten, 1982; Erosion Geological Strength Index (eGSI), after Pells et al 2016, and; Rock Mass Erodibility Index, after Douglas et al 2018). Interpreted values of eGSI are presented in Table 2. Detailed description of this Rock Mass Index is presented in Pells et al 2016, but in summary eGSI is calculated as the sum of GSI and eDOA, where GSI is the Geological Strength Index (after Hoek et al 1995) and eDOA is a Discontinuity Orientation Adjustment to account for increased erodibility from unfavourable orientation of rock mass defects.

Table 3 : Interpreted hydraulic indices for hydraulic domains

Parameter		HWG	WG	FG
GSI	Geological Strength Index (after Hoek et al 1995)	40	55	65-70
eDOA	Discontinuity Adjustment Orientation	-9	-3	-2
eGSI	Erosion Geological Strength Index	31	52	63-68

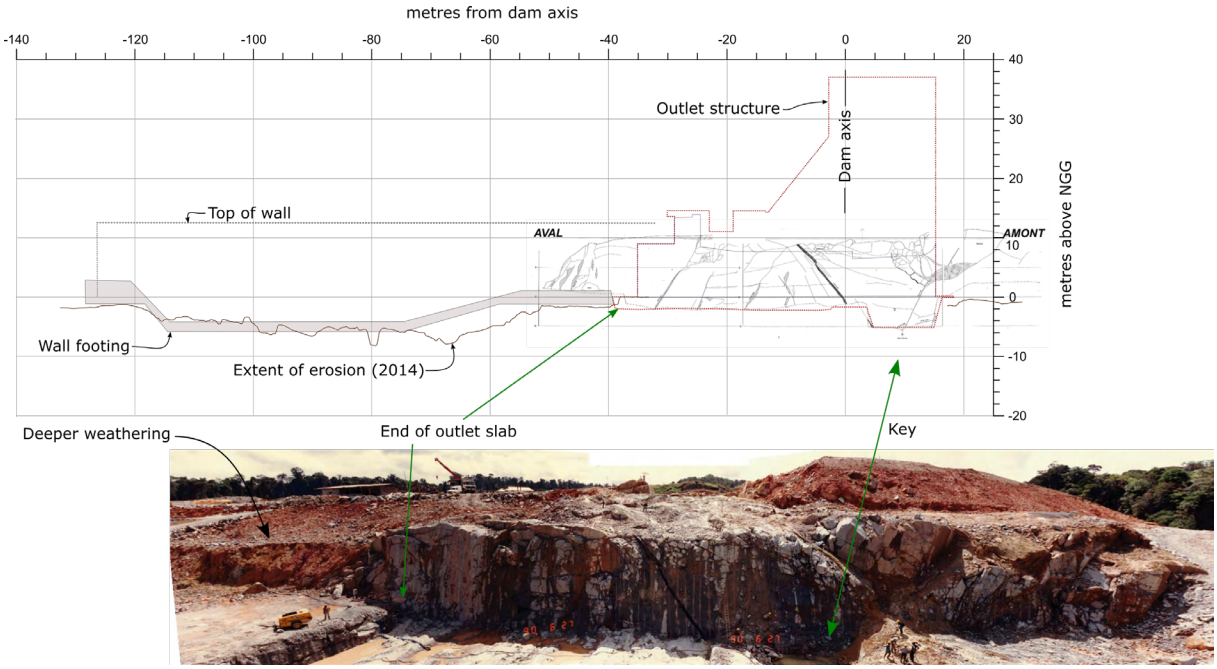

Figure 14: Previous mapping and photographs of geology – right wall of outlet.

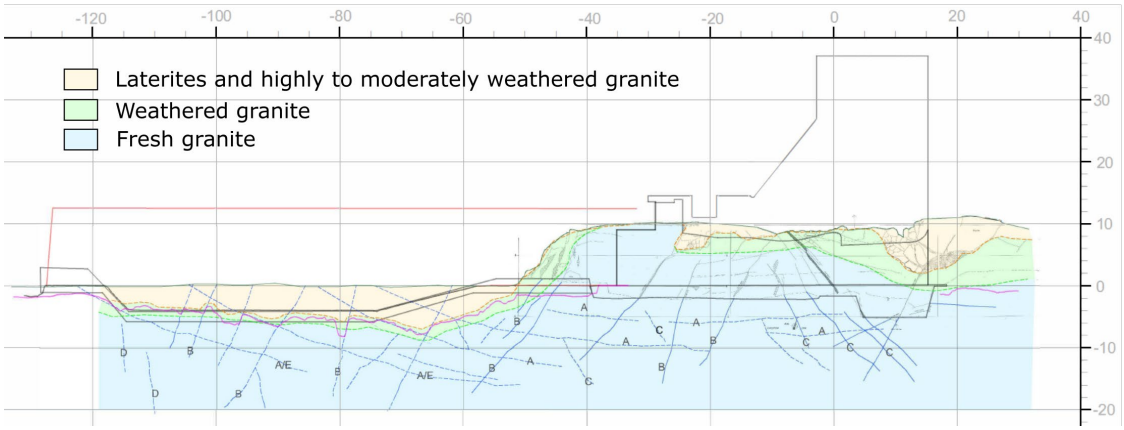

Figure 15: Example of interpreted stratigraphy.

3.5 Scour domains

Scour domains are regions with common geological and hydraulic conditions. Fifteen scour domains are defined by to the geological and hydraulic domains above (Table 3).

Table 4 : Interpreted scour domains

Rock type	Hydraulic domain				
	HD1	HD2	HD3	HD4	HD5
HWG	HWG-HD1	HWG-HD2	HWG-HD3	HWG-HD4	HWG-HD5
WG	WG-HD1	WG-HD2	WG-HD3	WG-HD4	WG-HD5
FG	FG-HD1	FG-HD2	FG-HD3	FG-HD4	FG-HD5

3.6 Scour assessment

Comparative scour assessment

Various methods have been published which allow an estimation of scour vulnerability of a rock mass based on comparison to case studies, where a rock-mass index is used to compare rock conditions and Π_{UD} is used to compare hydraulic conditions (van Schalkwyk et al 1994; Annandale 1995; Kirsten et al 2000; Pells et al 2016; Douglas et al 2018). These methods showed general agreement indicating that previously present HWG and WG domains would be subject to moderate to large erosion, but the remaining Fresh granite (FG) domains may experience minor to moderate erosion under future major spills. An example using eGSI (Pells et al 2016) for the existing chute (after removal of HWG) is shown in Figure 16. Results from the various comparative methods. Erosion classes in Figure 16 relate to the classification by Pells, 2016 which is reproduced in Table 5 below.

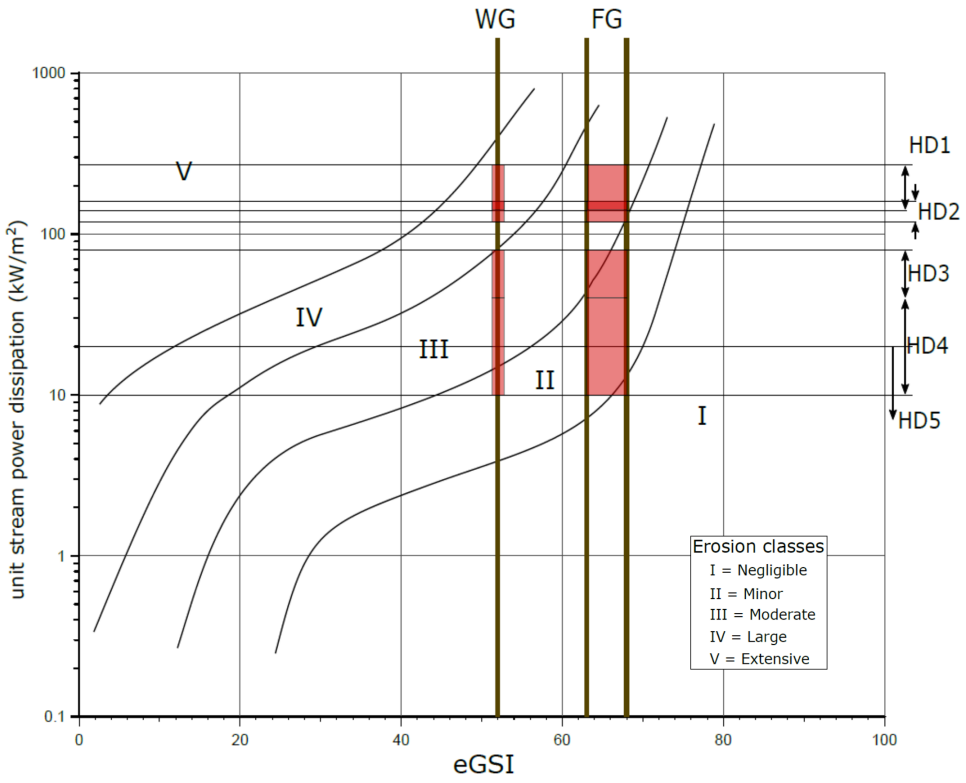

Figure 16: Comparative erosion assessment of existing spillway (Pells, 2016).

Table 5 : Erosion classes.

Erosion Class	Maximum erosion depth (m)	General erosion extent (m^3 per $100m^2$)	Descriptor
I	<0.3	<10	Negligible
II	0.3 to 1	10 to 30	Minor
III	1 to 2	30 to 100	Moderate
IV	2 to 7	100 to 350	Large
V	>7	>350	Extensive

Analytical scour assessment

Freebody diagrams were used to explore the kinematic stability of selected "blocks" across the spillway. Figure 17 (CFD Scenario 4) shows example blocks and their associated stability freebodies, through incorporation of time-averaged surface pressures predicted by the CFD model, and interpretation of the possible propagation of such pressures into defects in a manner similar to experimental results observed in Pells (2016). The uplift force on Block 1 is exceeded by the mass of the block suggesting that the block is kinematically stable under mean pressures. For Block 2 a more tenuous condition is seen, with a restraining force in excess of 148 kN required from strength of the defects to maintain stability. As hydraulic pressures are subject to fluctuation, larger pressure pulses potentially apply an impulse into defects, and have the capacity to displace the block, albeit momentarily. A timescale of gradual dislodging of the block is thus inferred by the passage of multiple pressure fluctuations over time.

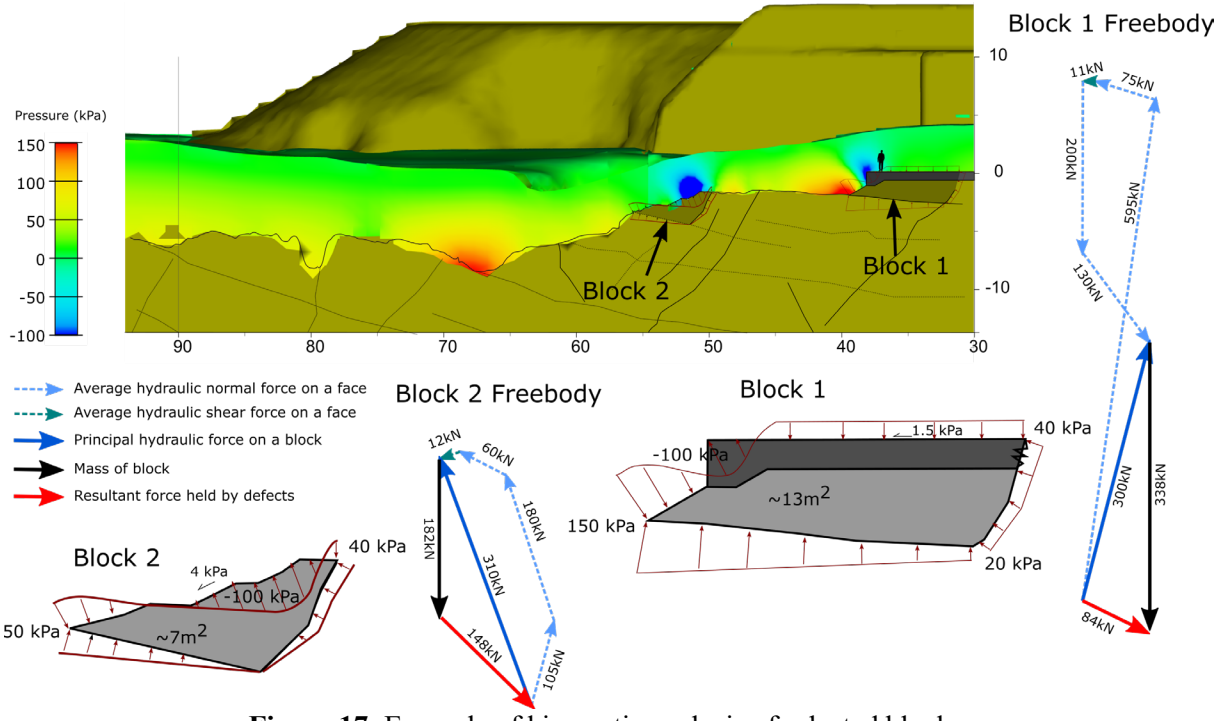

Figure 17: Example of kinematic analysis of selected blocks.

It is emphasized that these 2D free-bodies are approximations using a CFD grid that is course relative to block size and based upon interpretation of joint pressure propagation that follows patterns observed in laboratory tests. It is possible to undertake detailed calculations of pressure propagation into defects, but such calculations are also hostage to the assumption

of block size, as well as aperture, orientation and persistence of defects (all of which are unknown) and various assumptions about hydraulic conditions. Such calculations therefore do not liberate the practitioner from interpretative assumptions. The kinematic analyses serve to illustrate the perceived nature of erosion: the current scour hole is considered to be resistant to extensive erosion but the persistent fluctuating hydraulic conditions have the potential to incrementally strain blocks, ultimately allowing liberation of key blocks. This could then trigger further scour in episodes from time to time.

Coupled numerical scour assessment

Methods of coupled finite-element rock mass models and CFD modelling are currently being developed by the present writers. There was insufficient geological data at Petit-Saut to support this level of detailed analysis.

3.7 Risk evaluation

The comparative methods and interpreted geology indicate that weathered granite formations have been rapidly removed, forming a scour hole. The fresh granite that remains appears to be generally resistant to further erosion, although some risk of erosion could not be ruled out at the higher energy locations close to the outlet. This erosion is expected to be episodic in nature.

3.8 Protection measures

Options for hard engineering solutions would require extensive works for access and dewatering, and hence would be done most effectively at the one time. It was recommended that a remediation plan is formulated in anticipation of this time. Possible remediation options are:

- Dental concrete or underpinning of sections of the retaining wall
- Installation of dowels through the toe of the retaining wall to counteract sliding
- Installation of rock-bolts to tie together the rock mass
- Extension of concrete lining downstream with possible inclusion of flow guides or dissipator.

Some reduction in the rate of erosion may be achieved by gate operation patterns and modelling scenarios were examined to find conditions that may minimise energy expenditure.

3.9 Surveillance

Ongoing monitoring of the rock mass downstream of the bottom outlet was recommended. This would comprise repeated bathymetric surveys after two or three significant flow events, comprising typical operations of 50% to 100% opening of 1 or more gates. Surveys should endeavor to assess the extent of undermining of the wall footing.

4 CONCLUSION

The methodology for a “hydro-geological scour assessment” is demonstrated for the case study of scour at the bottom outlet to Petit-Saut dam, in French Guiana. The methodology provides a framework for systematic collation and analysis of data, application of available scour assessment tools, and encourages synthesis of independent geological and hydraulic analyses.

REFERENCES

Annandale, G.W., 1995. Erodibility. Journal of hydraulic research 33, 471–494.

Douglas K; Pells S; Fell R; Peirson W, 2018, 'The influence of geological conditions on erosion of unlined spillways in rock', Quarterly Journal of Engineering Geology and Hydrogeology, vol. 51, pp. 219 228, http://dx.doi.org/10.1144/qjegh2017-087

Hoek, E., P. K. Kaiser, and W. F. Bawden (1995): Support of underground excavations in hard rock, A.A. Balkema/Rotterdam/Brookfield.

Kirsten, H.A.D., 1982. Classification system for excavation in natural materials, in: Civil Engineer in South Africa. pp. 293–308

Pells, S.E., 2016. Erosion of Rock in Spillways (Doctoral Thesis). UNSW Australia, Kensington, N.S.W. http://handle.unsw.edu.au/1959.4/56008

Pells, S.E and Douglas, K. (in publication) “Hydro-geotechnical assessment of scour of rock”. Book chapter from an international workshop on behalf of the European Group of ICOLD and the French Committee on Dams and Reservoirs, Aussois, France, 11th to 14th December 2017

Pells, S.E. and Douglas, K.D 2019 “Guidelines for assessment of scour in unlined spillways” Proceedings from Africa 2019 - Conference of the International Journal of Hydropower and Dams, Windhoek, 2-4 April 2019 Aqua-Media International, London.

Pells S; Douglas K; Pells PJ N; Fell R; Peirson WL, 2016, 'Rock Mass Erodibility', Journal of Hydraulic Engineering, http://dx.doi.org/10.1061/(ASCE)HY.1943-7900.0001243

Pells, S.E., Peirson, W.L., Al-Qassab, F., 2021. “Guidance on the calculation of stream power dissipation for rock scour assessments”, in: Proceedings of the 10th International Conference on Scour and Erosion (ICSE-10). The International Society for Soil Mechanics and Geotechnical Engineering Geo-Institute of American Society of Civil Engineers, Virtual Oct 18-21. 2021, pp. 285–292.

van Schalkwyk, A., Jordaan, J.M., Dooge, N., 1994a. Die erodeerbaarheid van verskillende rotsformasies onder varierende vloeitoestande (No. WNK Verslag No. 302/1/95). verslag aan die waternavorsingskommissie deur die Departement of Geologie, Universiteit van Pretoria, South Africa.